

A DIGITALLY CONTROLLED AC TO DC POWER CONDITIONER THAT DRAWS SINUSOIDAL INPUT CURRENT

C. P. Henze
 Sperry Corp., U2S25
 P.O. Box 43525
 St. Paul, MN 55164

N. Mohan
 Univ. of Minn.
 Dept. of Elect. Eng.
 Mpls., MN 55455

ABSTRACT

An ac to dc power conditioner, which draws sinusoidal input current, is described and analyzed. Two control loops are used. The inner quantized-gain current program loop uses variable hysteresis to improve noise immunity. Digital proportional-integral control provides output voltage regulation by adjusting the gain of the current program loop.

1. INTRODUCTION

Recently there has been much interest in designing power conditioning equipment that draws sinusoidal input current from the ac line [1,2]. The step-up (boost) power conditioner described in this paper draws sinusoidal input current. The power conditioner has been designed to provide a regulated 220 Vdc output at 800 Watts when operating from a 120 Vac 60 Hz or 400 Hz line. Two control loops are used as shown in Figure 1. The current program loop controls the state of the power switch Q_1 to force the "instantaneous average" current in the inductor L_1 to follow the instantaneous rectified line voltage. Variable hysteresis control provides noise immunity by increasing the ripple current in the inductor when the instantaneous input voltage is high. Digital proportional-integral (PI) control provides output voltage regulation by adjusting, in discrete steps, the gain of the current program loop. A multiplying digital to analog converter (MDAC) serves as the interface between the voltage regulation loop and the current program loop. The sampling rate of the PI controller is determined by the input line frequency, allowing good transient response to be obtained at both 60 Hz and 400 Hz.

2. CURRENT PROGRAM LOOP

The function of the current program loop is to force the current drawn by the power conditioner to follow the input ac line voltage, thereby electronically emulating a resistor [3]. Several control laws may be used to generate the control waveform for the power switch. Among these control laws are: constant switching frequency control, constant current hysteresis control, variable current hysteresis control, and constant off-time control. The equations relating the inductor current ripple I_{r1p} and the switching frequency f_{sw} to the instantaneous average input voltage V_{in} (the

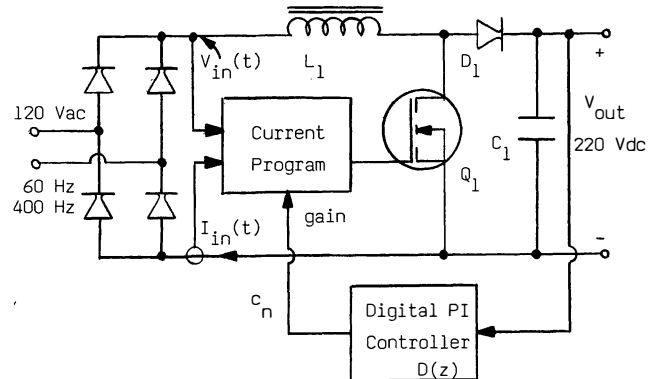


Figure 1. Two control loops are required for input current programming and output voltage regulation as shown in the block diagram of the digitally controlled power conditioner.

input voltage averaged over one switching period) and the dc output voltage V_{out} for the ideal step-up converter are derived in the appendix.

Experience has shown that noise generated by high speed switching can upset the operation of the current program loop [4]. An advantage of variable hysteresis control is that the highest noise immunity is provided when the switching energy (and therefore, the noise generation) is the greatest. The strategy of variable hysteresis control is to increase the peak-to-peak inductor ripple current I_{r1p} in proportion to the instantaneous rectified input voltage V_{in}

$$I_{r1p} = K_{hy} V_{in} \quad (1)$$

Since the switching frequency of the step-up converter is much higher than the ac line frequency, steady-state operation may be assumed in the step-up converter for any average instantaneous input voltage. Using Equation 1 and the approximations

$$t_{on} = \frac{L_1 I_{r1p}}{V_{in}} \quad t_{off} = \frac{L_1 I_{r1p}}{V_{out} - V_{in}} \quad (2,3)$$

an expression for the switching frequency f_{sw} may be found in terms of the current hysteresis coefficient K_{hy} , inductance L_1 , and input and output voltages

$$f_{sw} = \frac{V_{out} - V_{in}}{K_{hy} L_1 V_{out}} \quad (4)$$

The maximum switching frequency, which occurs when the input voltage goes to zero, is bounded and is given by

$$f_{sw,max} = (K_{hy} L_1)^{-1} \quad (5)$$

In practice, the maximum switching frequency will not be obtained since a real step-up converter is unable to maintain an output voltage as the input voltage and duty ratio approach zero.

The circuit of Figure 2 is used to implement the variable hysteresis current program loop. The MDAC multiplies a reference voltage V_{VLINE} (that is proportional to the instantaneous input voltage) by the quantized current gain value c_n (supplied from the PI controller in the voltage regulation loop) to provide an upper (or "turn-off") control voltage V_{cont1} . Resistive voltage division provides a lower (or "turn-on") control voltage V_{cont2} . The current flowing through the inductor L_1 is measured using a 0.1 Ohm resistor R_{sh} . The amplifier A_5 provides a voltage V_{IL} , that is proportional to the instantaneous inductor current, to the turn-on and turn-off comparators A_{4B} and A_{4A} . An S-R latch is toggled by the comparators to change the state of the switch Q_1 . The time relationship between V_{IL} , V_{cont1} , and V_{cont2} for one-half cycle of the input ac line is shown in Figure 3.

Transfer functions describing the gain of the current program loop and the current hysteresis coefficient in terms of the quantized current gain value and the input voltage will be useful in further analysis. The instantaneous voltages driving comparators A_{4A} and A_{4B} are related to the input voltage and inductor current through

$$\frac{V_{cont1}(t)}{V_{in}(t)} = \frac{R_2 R_4}{(R_1 + R_2) R_3} \frac{c_n}{2^m} \quad (6)$$

$$\frac{V_{cont2}(t)}{V_{cont1}(t)} = \frac{R_6}{R_5 + R_6} \quad (7)$$

$$\frac{V_{IL}(t)}{I_{L1}(t)} = \frac{R_{sh} R_8}{R_7} \quad (8)$$

where m is the number of bits used to represent the quantized current gain value c_n . During steady-state operation, the average of the upper and lower control voltages will be equal to the voltage representing the inductor current

$$\frac{V_{cont1} + V_{cont2}}{2} = V_{IL} \quad (9)$$

Therefore, the gain of the current program loop may be expressed as a function of the quantized current gain value

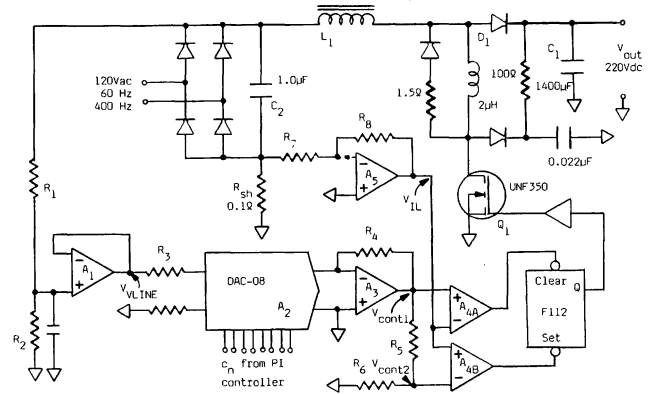


Figure 2. Variable hysteresis current program loop and snubber circuitry.

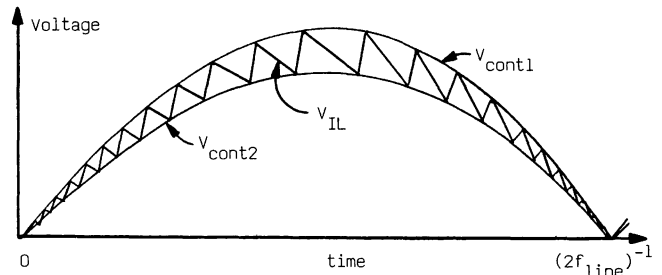


Figure 3. Control voltage waveforms in the current program loop during one half cycle of the ac line. The internal switching frequency is actually much higher than shown.

$$\frac{I_L(t)}{V_{in}(t)} = \frac{R_2 R_4 R_7 (0.5 R_5 + R_6)}{(R_1 + R_2) R_3 (R_5 + R_6) R_8 R_{sh}} \frac{c_n}{2^m} \quad (10)$$

The difference between the upper and lower control voltages, when multiplied by the voltage-to-current gain of Equation 8, determines the inductor ripple current

$$K_{hy} = \frac{I_{rip}(t)}{V_{in}(t)} = \frac{R_2 R_4 R_5 R_7}{(R_1 + R_2) R_3 (R_5 + R_6) R_{sh} R_8} \frac{c_n}{2^m} \quad (11)$$

The selection of capacitor C_2 is a critical aspect of the design of the unity power factor power conditioner. The capacitor conducts the ripple current directly to the shunt resistor, bypassing the ac line. If the capacitor is large and if there is no delay between the instant that the inductor current reaches a threshold and the instant that the power transistor Q_1 actually switches states, the current program loop will be unconditionally stable. However, if the capacitor C_2 is too large, unacceptable harmonic distortion will be produced in the ac line current.

3. VOLTAGE REGULATION WITH DIGITAL PI CONTROL

Digital proportional-integral (PI) control, implemented by the hardware circuit of Figure 4, is used for output voltage regulation [5]. A digital error amplifier, consisting of an uncompensated analog amplifier and an analog-to-digital (A/D) converter, samples and digitizes the error in the output voltage at each zero-crossing of the ac line to produce a digital error signal. Sampling at the zero-crossing is advantageous since the average output voltage (to a close approximation) is measured, regardless of the magnitude of the ripple component. Furthermore, sampling at the zero-crossings insures that no information will be obtained at the ripple frequency, thus preventing the voltage regulation loop from distorting the ac line current waveform in an attempt to reduce the output voltage ripple.

The digital output signal from the digital PI controller adjusts, in discrete steps, the gain of the current program loop, and is therefore termed the quantized current gain value. The quantized current gain value is restricted to the 2^m integer values which may be represented by an m -bit digital word. An eight-bit binary representation is used in our digital PI controller, allowing the decimal representation of the quantized current gain value c_n to range from 0 to 255. Since a hardware realization is used, the calculation updating the quantized current gain value is completed during the zero-crossings of the ac line.

The digital error signal e_n describes the difference between the actual output voltage of the power conditioner at the n th zero-crossing of the ac line and a reference voltage. Since an eight-bit two's complement representation is used in our digital PI controller, the decimal representation of e_n may range from -128 to +127, corresponding to an output voltage range of 240 V to 200 V.

The quantized current gain value c_n is calculated from the weighted summation of two digital signals. The first digital signal is proportional to the digital error input e_n . The second digital signal

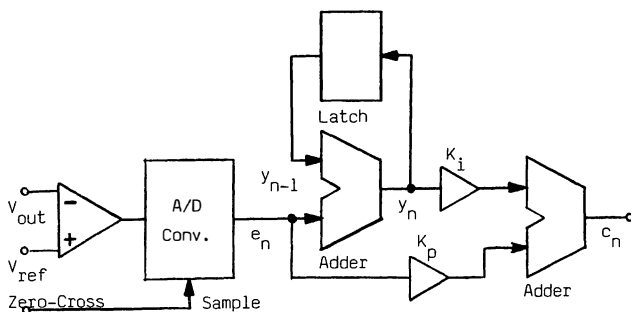


Figure 4. To provide output voltage regulation, the digital PI controller calculates the gain to be used by the current program loop during the next half cycle of the ac line from a digital error signal and the discrete integral of the digital error signal.

y_n is obtained from the discrete integration of the digital error input e_n . Discrete integration is accomplished using an adder and a register to maintain a continuous summation of the digital error input.

$$y_n = e_0 + e_1 + \dots + e_n \quad (12)$$

A discrete time difference equation may be written

$$y_n = y_{n-1} + e_n \quad (13)$$

Weighting coefficients K_p and K_i are provided to adjust the contribution of the proportional and integral signals to the current gain value calculation

$$c_n = K_i y_n + K_p e_n \quad (14)$$

Furthermore, overflow detection and correction is required at the outputs of both adders to prevent erroneous operation.

In general, K_p and K_i can take on any value. In our system however, K_p is restricted to unity and K_i may take on the values: 2, 1, 1/2, 1/4. This is because digital multiplication or division by powers of two is simply implemented, and because the gain of the digital error amplifier may be used to adjust the overall loop gain.

A discrete time domain representation of the PI controller is obtained by first taking the Z-transform of Equation 13

$$Y(z) = z^{-1}Y(z) + E(z) \quad (15)$$

$$\frac{Y(z)}{E(z)} = \frac{1}{1 - z^{-1}} \quad (16)$$

and substituting the result into the Z-transform of Equation 14

$$D(z) = \frac{C(z)}{E(z)} = K_i \frac{Y(z)}{E(z)} + K_p \quad (17)$$

The discrete time domain transfer function relating the quantized current gain signal to the digital error signal is

$$D(z) = \frac{C(z)}{E(z)} = \frac{K_p + K_i - z^{-1}K_p}{1 - z^{-1}} \quad (18)$$

The transfer function of the PI controller is first order. This is expected since the controller contains only a single delay element (used in the implementation of discrete integration).

4. COMPUTER SIMULATION

In order to maintain a unity power factor, the closed-loop frequency response of the output voltage regulation loop must cross through unity gain at a frequency which is less than the frequency of the ripple in the output voltage. If

this condition is not met, the output voltage regulation loop will distort the input current waveform in an effort to reduce the output ripple voltage. At frequencies less than twice the input ac line frequency, the current program loop may be absorbed into a single element. This allows a simple model of the digitally controlled power conditioner, shown in Figure 5, to be developed which is well suited for an iterative simulation using a personal computer.

Since the current program loop forces the rectified line current to follow the rectified line voltage, the low frequency model is driven from a digitally controlled current source

$$i_{in}(t, c_n) = \frac{I_{max} c_n}{2^n} \text{ABS}(\sin(\omega_{line} t)) \quad (19)$$

where I_{max} is a constant which defines the maximum peak input current, ω_{line} is the radian frequency of the ac line, and ABS denotes the absolute value operation. Using Equation 10, I_{max} is found as a function of the peak input voltage $V_{1n, pk}$

$$I_{max} = \frac{R_2 R_4 R_7 (0.5 R_5 + R_6)}{(R_1 + R_2) R_3 (R_5 + R_6) R_8 R_{sh}} V_{1n, pk} \quad (20)$$

For a time domain simulation, an iterative procedure is used to calculate the circuit voltages and currents through each half-cycle of the ac line. If the incremental time period T_{inc} (for which we use 1/200th of the period of the ac line) is sufficiently small, the voltage across capacitor C_1 as a function of time is discretely approximated using the equations

$$i_{load}(t) = v_{c1}(t) / R_{load} \quad (21)$$

$$i_{c1}(t) = i_{in}(t) - i_{load}(t) \quad (22)$$

$$v_{c1}(t + T_{inc}) = v_{c1}(t) + (i_{c1} T_{inc}) / C_1 \quad (23)$$

where the instantaneous input current $i_{in}(t)$ is defined in Equation 19. Once the ac line zero-crossing is reached, an updated quantized

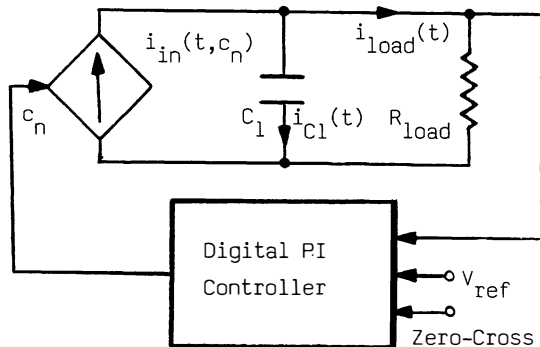


Figure 5. The current program loop is replaced by digitally controlled, time varying current source in the low frequency model of the digitally controlled power conditioner.

current gain value may be calculated from Equations 13 and 14 (and the transfer function of the digital error amplifier). The simulation may then continue for an additional half-cycle. Line and load transients may be simulated by making step changes in the parameters I_{max} and R_{load} .

5. VOLTAGE LOOP STABILITY

Typically, to determine if a closed-loop system is stable, a mathematical model of the system is developed and stability criteria are applied. The development of the closed-loop model is complicated in this case since the digital PI controller is easily described in the discrete time domain, whereas the (simplified) step-up converter is easily described in the Laplace domain. We will proceed by finding a discrete time domain description of the step-up converter, assuming that the step-up converter is driven by a zero-order hold current source [6]. Since the power conditioner is actually driven by a full-wave rectified waveform, a correction to the loop gain is required.

The action of the current program loop removes the pole due to inductor L_1 from the power conditioner transfer function. The Laplace domain transfer function of the simplified power conditioner circuit of Figure 5 contains only a single pole

$$G(s) = \frac{V_{out}(s)}{I_{in}(s)} = \frac{R_{load}}{s C_1 R_{load} + 1} \quad (24)$$

If it is assumed that the output (c_n) of the digital PI controller is a series of impulses and that these impulses define the output of a zero-order hold current source, a discrete time representation of $G(s)$ is found using

$$G(z) = Z(G_{ho}(s)G(s)) \quad (25)$$

where $G_{ho}(s)$ is the Laplace domain transfer function for the zero-order hold operation

$$G_{ho}(s) = s^{-1}(1 - e^{-Ts}) \quad (26)$$

and where T is the sampling period of the system (which is equal to half the period of the ac line). Using the definition of the Z transform, Equation 25 may be simplified

$$G(z) = \frac{z - 1}{z} Z \left[\frac{G(s)}{s} \right] \quad (27)$$

Consulting a Z transform table

$$\frac{a}{s(s + a)} \Leftrightarrow \frac{z(1 - e^{-Ta})}{(z - 1)(z - e^{-Ta})} \quad (28)$$

The discrete time domain transfer function of the simplified step-up converter is found using Equations 24 and 26.

$$G(z) = \frac{R_{load}(1 - \exp(-T/R_{load}C_1))}{z - \exp(-T/R_{load}C_1)} \quad (29)$$

The assumption has been made that the RC filter of the simplified step-up converter is driven by a zero-order hold current source. Therefore, we are assuming that a square pulse of current, for which the magnitude is updated at each zero-crossing of the ac line, is supplied to the RC filter. This is in fact, not the case. A correction may be made by adding a "dc" gain G_x to the closed-loop expression which accounts for the difference in output voltage that is produced by a single unit amplitude square current pulse and single unit amplitude half-sine current pulse, as illustrated by Figure 6. Circuit analysis shows

$$G_x = \frac{\frac{\omega}{RC} \left[\frac{e^{-T/RC}}{(\omega RC)^2 + \omega^2} + \frac{\sin[\pi - \tan^{-1}(\omega RC)]}{\omega((\omega RC)^2 + \omega^2)^{1/2}} \right]}{1 - e^{-T/RC}} \quad (30)$$

where: $C=C_1$, $R=R_{load}$, and $\omega=\omega_{line}$. If the RC time constant of the step-up is much larger than the period of the ac line, a simple expression is obtained.

$$G_x \cong \frac{1}{R_{load}C_1\omega_{line}\tanh[T/(2R_{load}C_1)]} \quad (31)$$

The expression may be further simplified

$$G_x \cong 1 - e^{-1} = 0.63 \quad (32)$$

Two other factors must be considered to determine the complete dc loop gain G_L . They are the gain associated with the digital error amplifier and the

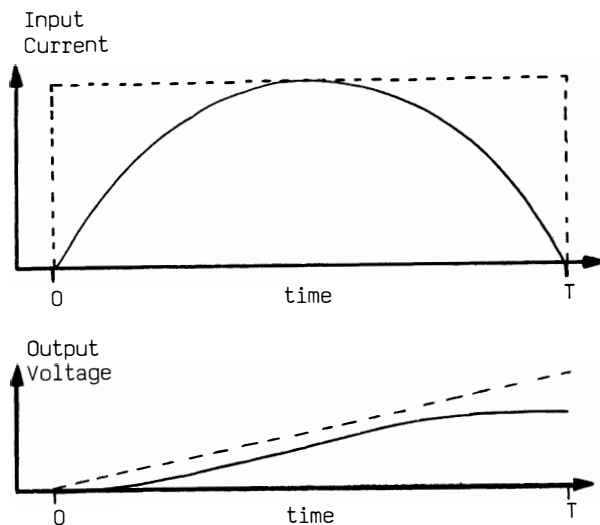


Figure 6. Since the output voltage that is produced at the sampling instant T by a unit amplitude square pulse is different than the output voltage that is produced by a unit amplitude half-sine pulse, a correction to the loop gain is required.

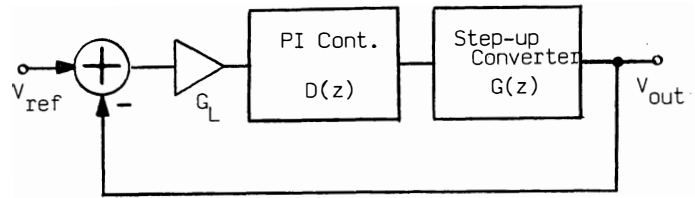


Figure 7. Low frequency closed-loop model of the digitally controlled power converter in the discrete time domain.

gain of the current program loop. The complete closed-loop dc gain G_L is given by

$$G_L = G_x \frac{e(\text{full-scale}) I_{max}}{V(\text{full-scale}) 2^m} \quad (33)$$

where $e(\text{full-scale})$ is the decimal value of the full scale digital error which occurs at the actual output error voltage of $V(\text{full-scale})$. As an example, evaluating Equation 33 for this power conditioner

$$G_L = (0.63) \frac{(127 \text{ units}) (10.4 \text{ Amps})}{(20 \text{ Volts}) (256 \text{ units})} = 0.16 \quad (34)$$

The closed-loop system may be represented in the discrete time domain by the block diagram of Figure 7. The digital PI controller transfer function $D(z)$ is given by Equation 18. The simplified step-up converter transfer function $G(z)$ is given by Equation 29 and the dc loop gain G_L is given by Equation 33. The closed-loop system will be stable if the roots of the polynomial $T(z)$ are located inside the unit circle.

$$T(z) = \frac{\text{Num}(z)}{\text{Den}(z)} = \frac{G_L D(z) G(z)}{1 + G_L D(z) G(z)} \quad (35)$$

After working through the algebra, the denominator of the closed-loop polynomial $T(z)$ is given by the second order expression

$$\text{Den}(z) = z^2 + z[G_L R(K_p + K_i)(1-A) - (1+A)] + A(1 + K_p G_L R) - K_p G_L R \quad (36)$$

where $R=R_{load}$ and $A=\exp(-T/R_{load}C_1)$. If the zeros of Equation 36 are inside the unit circle, closed-loop digitally controlled power conditioner will be stable. The zero locations will vary with: the proportional and integral weighting coefficients, the dc loop gain, the ac line frequency and voltage, the load resistance, and the output capacitance.

6. EXPERIMENTAL RESULTS

The ac line voltage and current waveforms obtained when the digitally controlled power conditioner is providing a 220 V output to a 100 Ohm load ($P_{out}=485 \text{ W}$) are shown in Figure 8. The ac line voltage was adjusted to 111.0 Vrms (using a variac)

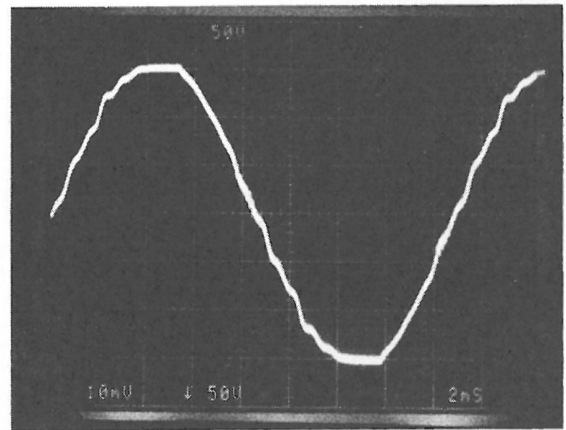
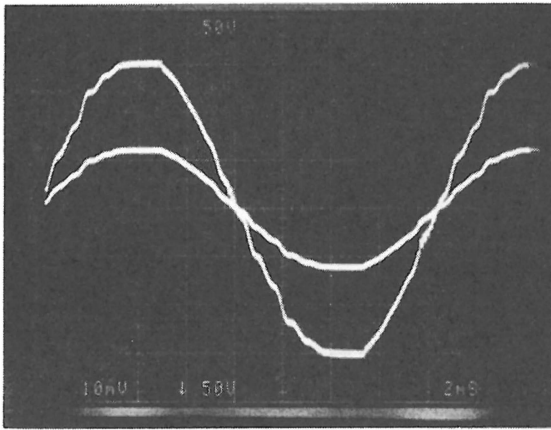


Figure 8. The ac line voltage and current waveforms, obtained when operating the digitally controlled power converter at an output power of 485 W, are closely matched. The ac line current is displayed at 5 A/div on the left and at 2 A/div on the right.

so that the amplitude of current and voltage waveforms would be equal when the current is displayed at 2 A/div. Unfortunately, a considerable amount of distortion was present in the ac power system at our facility; however, the close match between the voltage and current waveforms shows that the power conditioner draws resistive current from the ac line. In Figure 9, the harmonic current spectrum of the power conditioner is compared to the harmonic current spectrum obtained using a variable resistor adjusted for equal power dissipation. Ideally the power conditioner current spectrum would be identical to the resistor current spectrum; however, slight discrepancies are noted in the fifth and ninth harmonics of the spectra. A quantization effect--or quantization noise--is also noted in the second harmonic. The "fuzzy" line at 120 Hz is the result of the variation of the quantized current gain value c_n by +1, 0, or -1 at each zero-crossing of the ac line.

The digitally controlled power converter was also designed to accept a quantized current gain value from an external source, allowing open-loop operation. This feature will be used to examine the switching frequency versus voltage characteristics of the variable hysteresis current program loop. In Figure 10, the switching frequency is plotted against the normalized input voltage using a dc input power source and two different inductor values (of 1.09 mH and 361 μ H). Open-loop control was used with the quantized current gain value fixed to 128. Data was obtained by varying the load resistance while maintaining a constant output voltage of 220 V (squares) and by varying the load resistance while maintaining a constant input voltage of 100 Vdc (circles). The expected theoretical switching frequency characteristics, given by Equation 4, are also plotted. The maximum switching frequency, given by Equation 5, is not obtained since the step-up converter is not capable of producing a steady-state output voltage which is more than four times greater than the input voltage. Discrepancies between the experimental and

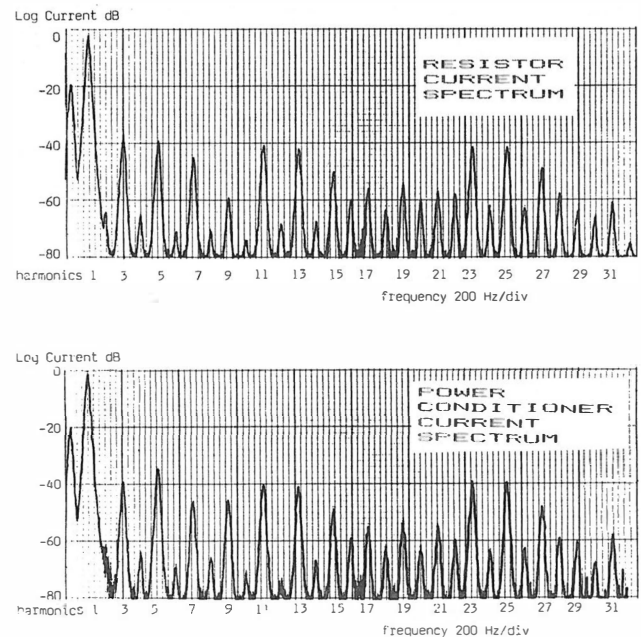


Figure 9. To demonstrate the resistive current characteristic of the power conditioner, the ac line current spectrum obtained with a variable resistor is compared to the ac line current spectrum obtained with the digitally controlled power conditioner.

theoretical results at high normalized input voltages are attributed to the non-ideal propagation delays and hysteresis (in comparators A_{4A} and A_{4B}) of the current program loop circuitry.

A single UNF350 is used as the power switching transistor. The drain voltage and inductor current waveforms are shown in Figure 11 for open-loop dc operating conditions of: $c_n=128$, $V_{in}=89.9$ V, and $V_{out}=218.5$ V. A low-loss snubber [4], shown in

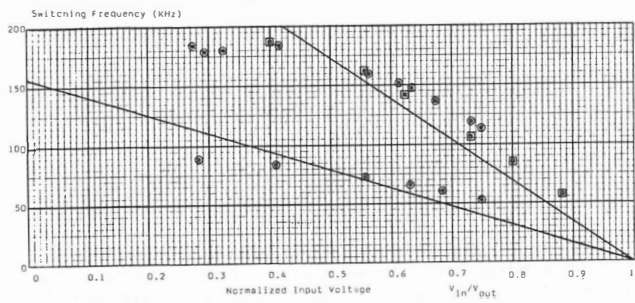


Figure 10. The actual and theoretical switching frequency is plotted against the normalized input voltage for inductor values of 1.09 mH and 361 uH.

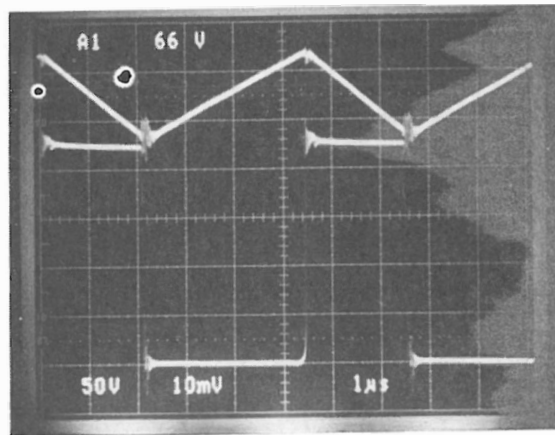
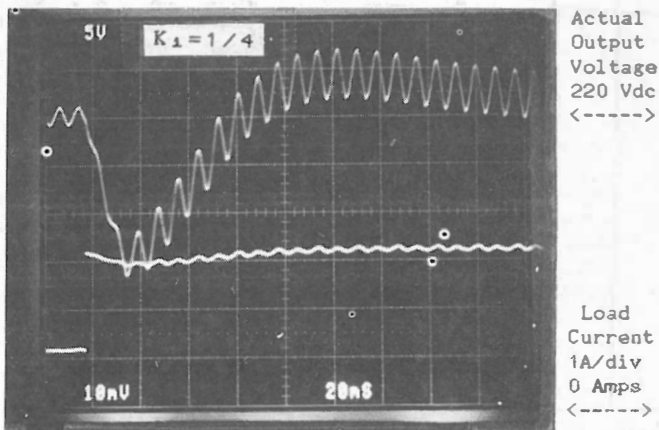


Figure 11. Drain voltage (50 V/div) and inductor current waveforms (0.5 A/div using the third line below center as the zero reference level) obtained using open-loop control at an input voltage of 89.9 V and an output voltage of 218.5 V.



Actual Output Voltage 220 Vdc
 Load Current 1A/div 0 Amps

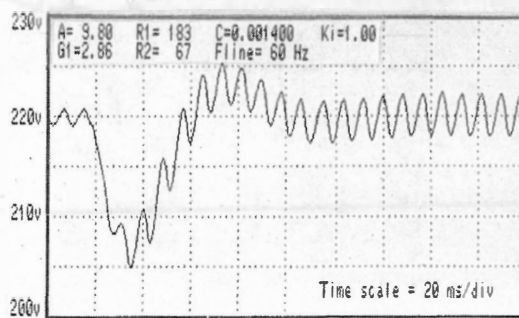
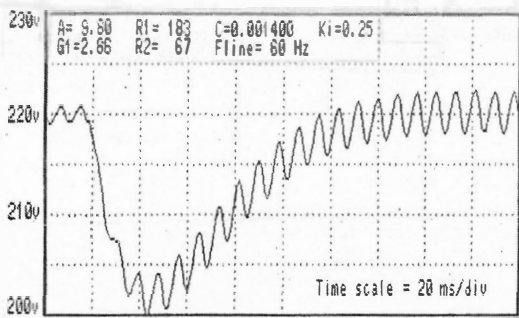
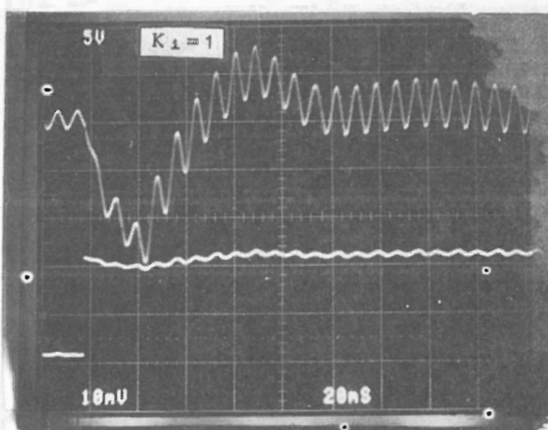


Figure 12. Actual and simulated output voltage response of the digitally controlled power conditioner to a step decrease in load resistance from 183 Ohms to 67 Ohms using integrator coefficients of 1/4 and 1.

Figure 2, was used and an efficiency of 96% was measured at an output power of 725 W. The turn-on switching transition was measured at 22 nsec and the turn-off switching transition was measured at 48 nsec.

The actual and simulated output voltage transient response to a step decrease in load resistance from 183 to 67 Ohms is shown in Figure 12 using integral weighting coefficients of $K_I=1/4$ and $K_I=1$. The resulting load current transients are also in the photographs of Figure 12. It is noted that the integrator coefficient can dramatically alter the transient response. The analysis of Section 5 indicates that the closed loop poles (using: $C_1=1400$ uF, $R_{load}=67$ Ohms, and $G_L=0.16$) are located at: 0.77 and 0.0048 for K_I of 1/4; and 0.046 +j0.040 for K_I of 1. The experimental and simulated results compare favorably but not exactly, indicating that the simple model described in Section 4 is incomplete. During transient response testing, it was noted that a 15 V peak deviation was produced in ac line voltage, suggesting that the power source characteristics should also be included to improve the accuracy of the simulation.

The digitally controlled power conditioner was modified for 400 Hz operation by the replacement of the 1400 uF output capacitor C_1 with a 200 uF capacitor. Figure 13 shows the output voltage transient response when operating from a 400 Hz source to a step decrease in load resistance from 200 to 100 Ohms using an integral weighting coefficient of 1/4. Because the decrease in the sampling time T is canceled by the decrease in the value of the output capacitor C_1 , the discrete time domain transfer function for the simplified step-up converter of Equation 29 is unchanged (to a close approximation since $400/60=6.67$, whereas

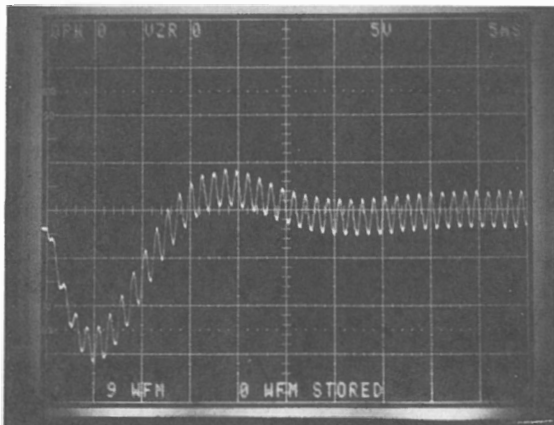


Figure 13. Actual output voltage response of the modified ($C_1=200$ uF) digitally controlled power conditioner, when operating from a 400 Hz source, to a step decrease in load resistance from 200 to 100 Ohms using an integrator coefficient of 1/4. The dc output voltage is 220 V.

$1400/200=7$.) Therefore, the closed-loop dynamics are automatically "speeded up" by a factor of 6.7 when the line frequency is changed from 60 to 400 Hz without requiring any change to the PI controller.

7. DISCUSSION

A high performance ac to dc power conditioner has been described and demonstrated which uses digital proportional-integral control for output voltage regulation and variable hysteresis control for current programming. A multiplying analog to digital converter is used as the interface between the voltage regulation loop and the current program loop. A stability analysis and a computer simulation technique have been presented.

The sampling instant of the digital PI controller is determined by the zero-crossings of the ac line. This scales the frequency characteristics of the closed-loop system with changes in the ac line frequency. Depending on the intended application, this may or may not be desirable. Power conditioners for different ac line frequencies are easily designed since only the output capacitor must be changed to take advantage of the improved dynamic characteristics offered by a higher line frequency. On-the-other-hand, if a single power conditioner is required to operate over a wide range of ac line frequencies, modifications are required to insure that proper operation is retained. This could be easily accomplished by including circuitry to automatically alter the proportional and integral weighting coefficients as different line frequencies are encountered. A second approach is to mask some of the zero-crossings when operating at higher line frequencies to maintain a nearly constant sampling rate. Providing an internal clock to determine the sampling instances if zero-crossings are not detected would allow the power conditioner to operate from dc as well as ac power sources. Care must be taken, however, since the loop gain varies with both magnitude and shape of the input voltage waveform.

The digital control technique is inherently well suited for three-phase applications since precise current balancing is easily obtained. A single PI controller and three step-up converters (with isolated dc to dc output stages) are required for a three-phase system. The digital quantized current gain control signal is easily delivered to each step-up converter, without any loss of accuracy, using, for example, digital optocouplers. This may be difficult in three-phase systems where analog multiplication is used between the the voltage regulation loop and the current program loops.

APPENDIX: Control Laws for the Step-up Converter

Four control laws may be used to develop the switch control waveform in the current program loop. These control laws are: constant switching frequency control, constant current hysteresis control, constant off-time control, and variable

current hysteresis control. The switching frequency and inductor ripple current are plotted against the normalized input voltage for each of the control laws in Figure A1. Derivations are given below using the symbols defined in Figure 1. It is assumed that the step-up converter is ideal and operating in steady-state.

Constant Frequency Control. Since the switching frequency is constant, the sum of the on-time and the off-time of the switch must also be constant

$$t_{on} + t_{off} = 1/f_{sw} = \text{constant} \quad (A1)$$

Assuming that the input and output voltages are constant over the duration of the switching cycle and using

$$V = L_1 \frac{di}{dt} \quad (A2)$$

the on-time and off-time may be expressed as

$$t_{on} = \frac{L_1 I_{rip}}{V_{in}} \quad (A3)$$

$$t_{off} = \frac{L_1 I_{rip}}{V_{out} - V_{in}} \quad (A4)$$

By substituting Equations A3 and A4 into Equation A1, an expression for the ripple current is obtained.

$$I_{rip} = \frac{V_{in}(V_{out} - V_{in})}{f_{sw} L_1 V_{out}} \quad (A5)$$

It is noted that the ripple current goes to zero when the input voltage is equal to zero and also when the input voltage is equal to the output voltage. The maximum ripple current may be found by setting the derivative of Equation A5, with respect to the input voltage, equal to zero.

$$\frac{dI_{rip}}{dV_{in}} = 0 \quad \text{when} \quad I_{rip} = I_{rip,max} \quad (A6)$$

$$I_{rip,max} = \frac{V_{out}}{4f_{sw} L_1} \quad \text{when} \quad V_{in} = \frac{V_{out}}{2} \quad (A7)$$

Constant Hysteresis Control. By definition, the ripple current will be constant. Using Equations A3 and A4, Equation A1 may be solved for the switching frequency

$$t_{on} + t_{off} = \frac{1}{f_{sw}} = \frac{L_1 I_{rip}}{V_{in}} + \frac{L_1 I_{rip}}{V_{out} - V_{in}} \quad (A8)$$

$$f_{sw} = \frac{V_{in}(V_{out} - V_{in})}{I_{rip} L_1 V_{out}} \quad (A9)$$

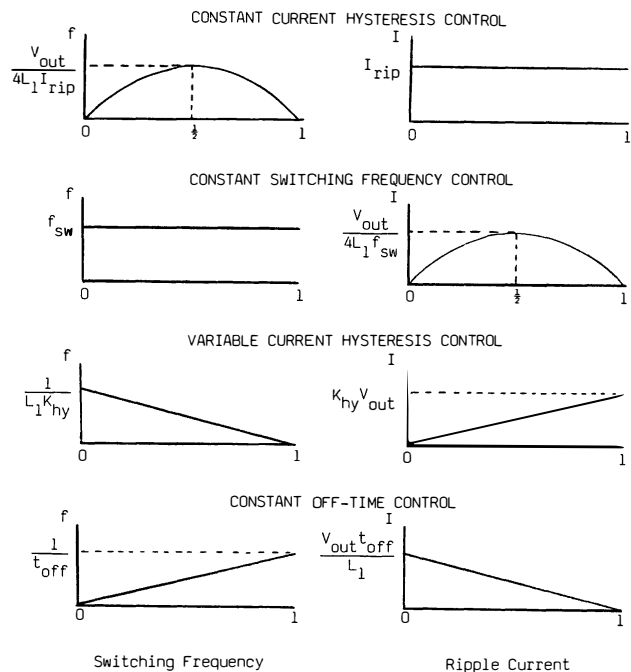


Figure A1. Switching frequency and inductor ripple current versus normalized input voltage (V_{in}/V_{out}) plots for various step-up converter control laws.

The switching frequency goes to zero as the input voltage goes to zero and when the input voltage is equal to the output voltage. The maximum switching frequency may be found by setting the derivative of Equation A9, with respect to the input voltage, equal to zero.

$$f_{sw,max} = \frac{V_{out}}{4L_1 I_{rip}} \quad \text{when} \quad V_{in} = \frac{V_{out}}{2} \quad (A10)$$

Constant Off-Time Control. Since the off-time is constant, the on-time may be expressed as

$$t_{on} = T_{sw} - t_{off} \quad (A11)$$

During steady-state operation, the static voltage transfer function for the step-up converter is

$$\frac{V_{out}}{V_{in}} = \frac{1}{1 - D} \quad (A12)$$

where D is the duty ratio of the power switching transistor. Since the duty ratio is defined as the on-time divided by the switching period T_{sw} , Equation A12 may be rewritten as

$$\frac{V_{in}}{V_{out}} = 1 - \frac{t_{on}}{T_{sw}} \quad (A13)$$

By combining Equations A11 and A13, the switching frequency may be solved for

$$f_{sw} = \frac{V_{in} - 1}{V_{out} t_{off}} \quad (A14)$$

The ripple current is found directly from Equation A4

$$I_{rip} = \frac{t_{off}}{L_1} (V_{out} - V_{in}) \quad (A15)$$

Variable Hysteresis Control. Expressions for the switching frequency and ripple current as a function of the input and output voltages are given in Equations 1 and 4 of the text. However, it is interesting to note that Equations 1 and 2 may be combined to show

$$t_{on} = K_{hy} L_1 = \text{constant} \quad (A16)$$

Therefore, variable hysteresis control could also be described as constant on-time control. In real implementations, slight differences would be expected in the switching frequency versus normalized input voltage characteristics since ideal operation is not obtained.

REFERENCES

- [1] E. Kamm, "New Military EMI Specifications Affecting the Input Architecture of AC to DC Converters," Proceedings of Powercon 8, 1981.
- [2] M. J. Kocher and R. L. Steigerwald, "An AC to DC Converter with High Quality Input Waveforms," IEEE PESC Conference Record; pp 63-75, 1982.
- [3] R. Keller and G. Baker, "Unity Power Factor Off Line Switching Power supplies," IEEE INTELEC Record; pp 332-339, 1984.
- [4] N. Mohan, T. M. Undeland, and R. J. Ferraro, "Sinusoidal Line Current Rectification with a 100KHz B-SIT Step-Up Converter, IEEE PESC Record; pp 92-98, 1984.
- [5] C. P. Henze and N. Mohan, "Modeling and Implementation of a Digitally Controlled Power Converter Using Duty Ratio Quantization," IEEE/ESA PESC Record, ESA Proceedings; pp 245-255, 1985.
- [6] B. C. Kuo, Digital Control Systems, Holt, Rinehart and Winston, New York; pp 108-111, 1980.